Published in final edited form as:
J Magn Reson Imaging. 2014 March ; 39(3): 641–647. doi:10.1002/jmri.24218.

Diffusion Tensor MRI of the Corpus Callosum in Amyotrophic Lateral Sclerosis

Molly C. Chapman, MA[1], **Laura Jelsone-Swain, PhD**[2], **Timothy D. Johnson, PhD**[3], **Kirsten L. Gruis, MD**[4,5], and **Robert C. Welsh, PhD**[2,6,*]

[1]Medical School, University of Michigan, Ann Arbor, Michigan, USA

[2]Department of Radiology, Medical School, University of Michigan, Ann Arbor, Michigan, USA

[3]Department of Biostatistics, School of Public Health, University of Michigan, Ann Arbor, Michigan, USA

[4]Department of Neurology, Medical School, University of Michigan, Ann Arbor, Michigan, USA

[5]Department of Neurology, Upstate Medical University, State University of New York, Syracuse, New York, USA

[6]Department of Psychiatry, Medical School, University of Michigan, Ann Arbor, Michigan, USA

Abstract

Purpose—To determine if decline in corpus callosum (CC) white matter integrity in patients with amyotrophic lateral sclerosis (ALS) is localized to motor-related areas.

Materials and Methods—Twenty-one ALS patients and 21 controls participated. Diffusion tensor images (DTI) were acquired using 3 Tesla (T) MRI. Tract-based spatial statistics were used to examine whole-brain white matter damage. A segmentation schema was used to define CC volumes-of-interest (VOI). Fractional anisotropy (FA) and radial- and axial-diffusivity (RD, AD) were extracted from VOIs and compared between groups. DTI measurements in motor-related Area III were tested for correlation with symptoms and disease duration.

Results—Extracted FA values from CC VOIs were reduced in ALS patients ($P \leq 0.0001$), particularly in Areas II and III ($P \leq 0.01$). Reduced FA in Area III correlated with disease symptomology ($P \leq 0.05$) and duration ($P \leq 0.02$). Between-group whole-brain comparisons ($P \leq 0.05$, corrected) showed reduced FA and increased RD throughout white matter regions including the CC, corona radiata, and internal capsule. AD was increased in the left corona radiata and internal and external capsules.

Conclusion—FA in motor-related regions of the CC is more affected than other CC areas in ALS patients. Microstructural pathology of transcallosal fiber tracts may represent a future component of an imaging biomarker for ALS.

Keywords

DTI; corpus callosum; amyotrophic lateral sclerosis

[*]Address reprint requests to: R.C.W., Medical Science I, Room 3208C, Department of Radiology, University of Michigan, 1301 Catherine Street, Ann Arbor, MI. rcwelsh@med.umich.edu.
Dr. Gruis is now at SUNY, Upstate, Syracuse NY.

AMYOTROPHIC LATERAL SCLEROSIS (ALS) is a progressive neurodegenerative disease affecting both upper- and lower-motor neurons. There are active efforts in the field of neuroimaging to discover a biomarker to aid in earlier diagnosis, improve the understanding of motor-neuron degeneration, and perhaps serve as an outcome measure for disease-modifying therapies. Unfortunately, early diagnosis of ALS has proven elusive as clinical confirmation can only occur after both upper (UMN) and lower motor neuron (LMN) involvement are detected by neurologic examination, which often occurs at a time point of advanced pathology (1). While noninvasive neurophysiologic techniques exist to detect subclinical LMN dysfunction, there is no sensitive tool that can similarly distinguish UMN dysfunction to aid in early diagnosis (2). For these reasons, much attention has turned toward neuroimaging as a means of identifying UMN involvement (3).

Particular interest in the use of diffusion tensor imaging (DTI) to identify UMN involvement in ALS has been growing. DTI research to date has largely replicated findings from postmortem studies indicating widespread microstructure deterioration along the UMNs of the corticospinal tract and corpus callosum (CC), validating this method as a valuable in vivo marker of the disease process (4–7). The CC in patients with ALS has consistently shown DTI changes, with decreased fractional anisotropy (FA) and increased radial and axial diffusivity (RD, AD) compared with control subjects (8). These changes may correspond to degeneration of transcallosal fibers passing between primary motor cortices observed at 1.5T (9). However, it has yet to be determined whether the mid-body motor fibers of the CC are more strongly affected in ALS when compared with other portions of the CC.

The goal of our study was to systematically test the hypothesis that transcallosal fibers passing between primary motor cortices are especially affected compared with other regions of the CC using DTI. We examined the relationship between this microstructural measure and clinical evaluation of disease status. Additionally, we used tract-based spatial statistics (TBSS) to examine the whole-brain pattern of white matter changes. We highlight this point as TBSS-based normalization removes placement variance as seen in previous work using VOIs or tracking seed locations defined in patient space (10,11). Finally, this present work was performed at 3.0T compared with 1.5T in previous work (9), and DTI at this higher field strength has been shown to have increased signal to noise ratio in areas such as the CC and corticospinal tract (12).

MATERIALS AND METHODS

Study Participants

Patients diagnosed with definite ALS by a neuromuscular physician using El Escorial criteria were recruited from and followed by the Motor Neuron Disease Center. Twenty-one ALS patients (13 male; mean age, 59.8 years), 15 with limb-onset ALS (11 male; mean age, 58.6 years) and 5 patients with bulbar-onset ALS (2 male; mean age 63.4 years), were included in the study. All patients were ambulatory; did not have hemiplegia, dysphagia, dyspnea, or respiratory failure; and were without other neurologic or psychiatric disease. Patients with ALS were compared with 21 healthy controls without psychiatric or neurologic disorders (11 male; mean age, 56.5 years). Controls were recruited from the local community by flyer and Internet advertisements. A portion of these participants were involved in a previous published study (13). The University of Michigan Medical School Institutional Review Board approved this study, and all participants gave written informed consent before their participation in any part of the investigation.

Clinical Measures

The revised ALS Functional Rating Scale (ALSFRS-r), a 12-question validated rating instrument with a maximum score of 48, was administered to all patients within 7 days of their scanning session to assess motor function (14). The Edinburgh Inventory was used to determine hand dominance (15). Hand strength was measured with a hand-grip dynamometer averaged across three trials on both hands. Hand strength disparity was recorded as the absolute value of the difference between dominant and nondominant hand strength.

Image Acquisition

MRI of all patients and controls was acquired using a GE 3T Excite 2 scanner (General Electric, Milwaukee, WI). Three-plane localizer images were acquired, followed by a 40 slice T_1-weighted anatomic overlay (echo time, TE = 5.7 ms; repetition time, TR = 250 ms; 220 mm field-of-view, FOV; 256 × 256 matrix; 3 mm slice thickness). Subjects lay resting for a 5-min diffusion tensor scan (echo-planar imaging, 220 mm FOV, 128 × 128 matrix, TE = 70 ms, TR = 9000 ms, b = 800 s/ mm^2). Within each scan, a b = 0 image and 15 noncollinear diffusion-weighted images were collected (16).

Diffusion Tensor Imaging

Preprocessing—All DTI processing was done using FSL version 4.1.9 (17,18). Images were corrected for head motion and eddy currents. Field maps were acquired with a spiral sequence in the same spatial locations as the diffusion-weighted images. These field maps were used to unwarp the diffusion-weighted images due to the echo-planar imaging readout of the DTI sequence. The final corrected images were used to calculate tensor elements. The tensor elements were subsequently used to determine FA, AD, and RD (16,19).

Tract-Based Spatial Statistics—Voxel-wise statistical analyses of all three DTI maps were carried out using tract-based spatial statistics (TBSS v1.2) (20), a part of FSL. Whole-brain, voxel-wise group comparison was then performed using a permutation-based nonparametric inference t-test within the general linear model framework using 10,000 permutations (21). T-value maps were augmented using threshold free cluster enhancement (22) and considered significant at $P \leq 0.05$.

Corpus Callosum VOI Drawing and DTI Extractions From CC Regions

A standard mask was drawn of the CC to extract DTI metrics from individual DTI maps in the following manner. Anatomical imaging data from this cohort indicate that gross size differences do not exist between these patients and healthy controls (23). Therefore, a single mask was drawn guided by the FMRIB58 template in MNI space in the mid-sagittal slice for application to all subjects' data. The whole CC mask was auto-segmented using an in-house MATLAB program (MATLAB, MathWorks Inc. R2011b), described previously (23). This CC mask was then segmented geometrically with another in-house MATLAB program into five sub-regions as defined by Hofer (24) (their Fig. 3). The Hofer interpretation of this data, guided by tractography in human subjects, takes into account findings that suggest fibers connecting the primary motor cortices are more posterior in humans than in primates. These segmented regions were functionally defined as: Area I, the region that connects the caudal orbital prefrontal, inferior premotor cortices, and prefrontal cortices; Area II, the region that connects the premotor, cingulate motor, presupplementary and supplementary motor areas; Area III, the primary focus of this analysis, contains the fibers that connect the primary motor cortices; Area IV, connecting primary sensory cortices; and Area V, containing superior temporal, posterior parietal, occipital, and inferior temporal cortex fibers (24).

Each of the five CC areas was expanded to the right and left along the X-axis by 8 mm, constrained to the FMRIB58 template. The subsequent VOI of the CC regions were eroded to minimize partial volume effects on values located on the edges of the VOI. These final CC area masks were used to extract FA, AD, and RD values from TBSS-registered nonskeletonized whole-brain data.

ANCOVA Using DTI by CC Region

An analysis of covariance (ANCOVA) was performed to test for a main effect between patient group membership incorporating all DTI changes within the CC. Given the wide range of age in both comparison groups, age was included as a covariate in the model. This analysis was performed separately with mean FA, RD, and AD values. Results were considered significant at a nominal significance level, α, set to 0.05. In the ANCOVA analyses yielding a significant effect, post hoc, two-tailed independent sample t-tests of DTI mean extracted values were performed to compare microstructural changes in all five CC areas and thus confirm which CC areas are most affected. Results were considered significant for *P* values below a Bonferroni-corrected α of 0.01. Importance of CC-area contribution to change in the CC was determined by the magnitude in CC-area change between groups.

Correlation Analysis Between Structural and Clinical Measures of Disease Severity

Driven by our hypothesis that CC Area III would be most affected by motor neuron degeneration compared with other CC regions, a targeted analysis of the relationship between DTI measures in Area III and clinical measures was performed in the patient group. A partial correlation analysis was conducted with age controlled in each comparison. These clinical measures include the ALSFRS-r cumulative score, disease duration defined by months since symptom onset, and hand strength disparity. Correlation coefficients were considered significant at a level of $\alpha = 0.05$ using a two-tailed test. All clinical correlations were carried out in SPSS release version 20.0.0 (SPSS Inc., an IBM Company, 1989, 2010).

RESULTS

Group Demographics and Clinical Data

Group averages are presented in Table 1, and individual patient data are shown in Table 2. Because many of the limb-onset patients did not identify lateralization of symptom onset (see Table 2), analysis of MR results proceeded without image mirroring as performed in recent neuroimaging studies (8).

TBSS DTI: Decreased FA and Increased AD & RD in ALS Patients

All DTI differences described below are significant ($P \leq 0.05$, corrected for multiple comparisons). The ICBM-DTI-81 white-matter labels atlas (25) was used to describe anatomical locations of DTI changes.

FA was significantly reduced in the ALS patient group compared with healthy controls in the body and genu of the CC, extending bilaterally. Along the CST, FA differences were seen in the superior corona radiata bilaterally and the anterior corona radiata descending into the internal capsule on the left side. FA was reduced in the left superior longitudinal fasciculus. RD was significantly increased in ALS patients. Specifically, the body and genu of the CC showed increases in RD, which extended laterally to the right and left. In the CST, bilateral increases in RD were present in the superior corona radiata extending caudally through the posterior limb of the internal capsule and into the midbrain. On the left side, these changes descended further to the base of the pons. Increases in AD in the patient group

were localized to the left superior corona radiata and the left internal and external capsules. Thalamic tracts were involved bilaterally and reached caudally to the level of the midbrain on the left. There was also some involvement of the left superior cerebellar peduncle. See Figure 1 for FA, RD, and AD results. These results are in line with previous findings in the literature (26–28).

Given the striking difference in FA and RD maps with regard to extent of white matter involvement, we conducted a post hoc voxel counting of whole-brain binary images generated for FA and RD and the union of resulting images to calculate the ratio of white-matter involvement given by FA and RD, respectively. We generated binary suprathreshold masks of RD and FA at the following *P* values: 0.075, 0.0625, 0.050, 0.0325, 0.0250 and calculated the mean and variance of the observed ratio. The results of this exercise indicated that the extent of white-matter involvement as measured by RD is approximately twice that as measured by FA ($N_{RD}/N_{FA} = 1.985 \pm 0.192$).

ANCOVA of CC Extracted Mean Values

Because no differences were seen in the TBSS results above with respect to AD in the CC, only FA and RD were tested in the ANCOVA analyses. FA values demonstrated a significant main effect of group ($P = 4.2 \cdot 10^{-6}$) (Fig. 2). Post hoc t-tests yielded significant differences between healthy controls and patients in Areas II ($t = -2.83$, $P = 0.0072$) and III ($t = -3.00$; $P = 0.0047$). Based upon CC-area mean effect size, order of importance of CC-area contribution to the main effect was Area III ($\Delta FA_{III} = 0.063$) and then Area II ($\Delta FA_{II} = 0.047$). The ANCOVA for RD values also showed a significant main effect of group ($P = 1.6 \cdot 10^{-5}$) (Fig. 2). Post hoc t-tests of RD showed significant difference between healthy controls and patients in Areas I ($t = 2.88$, $P = 0.0063$), II ($t = 3.62$, $P = 0.0008$), III ($t = 2.72$, $P = 0.0096$), and V ($t = 3.00$, $P = 0.0047$).

Mean FA and RD Values in Area III Correlate With Clinical Measures

Results from the partial correlation between Area III mean FA and ALSFRS-r scores showed a significant relationship, with decreasing FA corresponding to worsening ALSFRS-r scores ($r = 0.457$, $P = 0.043$) (Fig. 3). Mean Area III FA also correlated negatively with disease duration ($r = -0.524$, $P = 0.018$) (Fig. 3). There was no significant correlation with FA and hand strength difference ($r = 0.408$, $P = 0.074$). RD values in Area III correlated positively with disease duration ($r = 0.621$, $P = 0.003$) but not with ALSFRS-r scores ($r = -0.351$, $P = 0.129$) or hand strength difference ($r = -0.335$, $P = 0.148$).

DISCUSSION

The present investigation aimed to systematically examine diffusion properties of motor-specific functional regions of the CC, guided by the well-defined geometric scheme of Hofer and Frahm (a modification of an earlier segmentation scheme of Witelson) (24,29) in patients with ALS. The results confirm our hypothesis that white matter deterioration within the CC converges on transcallosal primary motor cortex fibers, designated Area III. Notably, our study also demonstrated decreased FA in the CC of patients with ALS, which was driven by changes in the transcallosal regions connecting fibers between the premotor, cingulate motor, presupplementary and supplementary motor areas, collectively represented by Area II. These results provide more convincing evidence than previously available that the degeneration of white matter within the CC is localized to motor-specific regions.

While various DTI studies have flagged the CC as an important location in the extra-motor network of pathology in ALS, only one thus far has systematically addressed the location within the CC of this damage. This study linked FA changes with Area III in ALS patients,

but did not attempt to statistically differentiate the contributions of the various functional sub-areas of the CC (9). For this reason, our results are noteworthy in finding the motor-related regions of the CC most significantly affected. This significant finding has important clinical value for the following reasons.

It has been stated that there is a need for an objective early marker for UMN impairment in ALS. Using the current clinically guided methods of diagnosis, disease-related neurodegeneration outside the traditional motor network of the CST is not easily observed (2). A notable exception is the mirror movement, an involuntary movement that mirrors that of a contralateral limb. It is considered a clinical sign of transcallosal fiber dysfunction and has been observed in some ALS patients (30). The presence of this sign is likely related to white matter changes in motor regions of the CC. Sub-clinical forms of the sign can be elicited by applying transcranial magnetic stimulation to the primary motor cortex and measuring neuronal excitability in the ipsilateral limb. Studies with this technique showed an altered response in both definite and probable ALS patients earlier in the disease process (30). This indicates that the CC, in particular Area III, may be involved early in the disease process. The focus of that study, callosal dysfunction, relates directly to the aims of the present investigation. Through our study, we aimed to draw an important connection between Wittstock's peripherally measured functional phenomena and our centrally observed loss of CC structural integrity. Such comparisons may shed more light onto the role of callosal dysfunction in the disease process.

The clinical significance of our data is further supported in finding correlations between white matter changes in the patient group and measures of disease status. Specifically, patients with lowest FA in Area III were also those with the greatest disease severity and symptom duration. These findings indicate that DTI changes in Area III potentially represent an objective marker of more symptomatic disease. For this observation to be validated as a transitional sign of ALS progression, more direct comparisons should be approached with larger group sizes between high-functioning and low-functioning patients in addition to longitudinal studies.

Sub-region analysis of the CC in ALS warrants further investigation, especially in light of previous resting state functional connectivity MRI studies that may reflect the functional sequelae of destructive processes ongoing in this region (13,31,32). With the goal of developing a multimodal approach to defining an early biomarker in ALS, future studies should also combine these functional, structural, and other imaging modalities to shed light onto the role of this transcallosal fiber tract.

Another important finding was the qualitative observation that differences in RD between patients and controls appear to represent a more widespread network of disease involvement than FA differences. This effect is echoed by the finding that there are significant group differences in RD of the CC that extend beyond Areas II and III. From the present analysis, it is challenging to hypothesize why, at a cellular level, RD may be more sensitive to ALS pathology than FA. Comparisons of DTI data and corresponding histologic observations indicate that increases in RD may represent myelin degeneration, whereas decreases in AD correspond more to axonal injury, and decreases in FA do not distinguish between the two types of neurodegeneration (33). This together with the results of our study may suggest that a demyelinating process is more widespread in white matter in ALS. This idea conflicts with postmortem reports indicating that alterations in motor neuron cell bodies and axonal processes are at least as prominent as observations of demyelination (4). However, our observation of increased AD, also recently seen in ALS (34,35), could be indicative of axonal loss. Future advances in the understanding of the histologic correlates of different DTI metrics would serve well to inform this discussion.

One shortcoming of these data is that it is unclear whether callosal involvement in the disease might predate clinical evidence of the disease that physicians currently use to make the diagnosis. Indeed, recent longitudinal DTI data suggest that changes within the corpus callosum may not be a sensitive reflection of disease progression (35). The timing of callosal involvement in ALS clearly requires further study and certainly capturing DTI data in ALS patients earlier in the disease process will help elucidate that involvement. Where possible, it is also suggested that DTI data be collected in patients presenting with symptoms but as yet diagnosed with definitive ALS.

In conclusion, this study has provided evidence that motor and supplementary motor cortex-associated tracts of the corpus callosum are especially affected by the ALS disease process. A recent meta-analysis by Foerster et al (36) demonstrated the limited diagnostic utility of DTI, however, this analysis was limited to mainly white matter regions outside the corpus callosum and excluded approaches for whole brain analysis as we have done here. DTI examination of FA in this region may be incorporated into a neuroimaging biomarker, which could provide a more objective test of UMN impairment and allow for earlier detection of disease. Additionally, reduced FA in this region is indicative of greater disease severity and duration, however previous longitudinal studies have not identified a progressive change in this region over time. It could be postulated that early white matter involvement in Areas II and III represented by FA decreases could therefore be predictive of clinical prognosis, which ultimately would allow for increased enrollment in clinical trials, and more importantly, earlier targeted clinical management. Finally, although a qualitative observation, the more extensive involvement of white matter as measured by RD may implicate RD as a more sensitive measure of the ALS disease process than FA.

Acknowledgments

Contract grant sponsor: NIH/NINDS; Contract grant number: NSR01–052514.

The authors thank all participants for their time volunteered for this study. We also thank Donald McNair, Rebecca Hovatter, and Pooja Modi for their assistance in data collection. We would like to thank Dr. Bradley Foerster for reading an earlier version of this manuscript. The aforementioned authors have no disclosures of competing financial interests to make regarding this work. R.C.W. was funded by a Basic Radiological Science Award and the NIH/NINDS R01NS052514.

References

1. Gelb, DJ. Introduction to clinical neurology. New York: Oxford University Press; 2011. p. 1
2. Elliott JL. A clearer view of upper motor neuron dysfunction in amyotrophic lateral sclerosis. Arch Neurol. 1998; 55:910–912. [PubMed: 9678307]
3. Turner MR, Grosskreutz J, Kassubek J, et al. Towards a neuroimaging biomarker for amyotrophic lateral sclerosis. Lancet Neurol. 2011; 10:400–403. [PubMed: 21511189]
4. Lawyer T, Netsky M. Amyotrophic lateral sclerosis. AMA Arch Neurol Psychiatry. 1953; 69:171–192.
5. Smith MC. Nerve fibre degeneration in the brain in amyotrophic lateral sclerosis. J Neurol Neurosurg Psychiatr. 1960; 23:269–282. [PubMed: 21610893]
6. Brownell B, Oppenheimer DR, Hughes JT. The central nervous system in motor neurone disease. J Neurol Neurosurg Psychiatry. 1970; 33:338–357. [PubMed: 5431724]
7. Turner MR, Kiernan MC, Leigh PN, Talbot K. Biomarkers in amyotrophic lateral sclerosis. Lancet Neurol. 2009; 8:94–109. [PubMed: 19081518]
8. Filippini N, Douaud G, Mackay CE, Knight S, Talbot K, Turner MR. Corpus callosum involvement is a consistent feature of amyotrophic lateral sclerosis. Neurology. 2010; 75:1645–1652. [PubMed: 21041787]

9. Müller H-P, Unrath A, Huppertz HJ, Ludolph AC, Kassubek J. Neuroanatomical patterns of cerebral white matter involvement in different motor neuron diseases as studied by diffusion tensor imaging analysis. Amyotroph Lateral Scler. 2012; 13:254–264. [PubMed: 22409361]
10. Cosottini M, Giannelli M, Siciliano G, et al. Diffusion-Tensor MR Imaging of corticospinal tract in amyotrophic lateral sclerosis and progressive muscular atrophy. Radiology. 2005; 237:258–264. [PubMed: 16183935]
11. Wang S, Poptani H, Woo JH, et al. Amyotrophic lateral sclerosis: diffusion-tensor and chemical shift MR imaging at 3. 0 T. Radiology. 2006; 239:831–838. [PubMed: 16641339]
12. Polders DL, Leemans A, Hendrikse J, Donahue MJ, Luijten PR, Hoogduin JM. Signal to noise ratio and uncertainty in diffusion tensor imaging at 1.5, 3.0, and 7. 0 Tesla. J Magn Reson Imaging. 2011; 33:1456–1463. [PubMed: 21591016]
13. Jelsone-Swain LM, Fling BW, Seidler RD, Hovatter R, Gruis K, Welsh RC. Reduced interhemispheric functional connectivity in the motor cortex during rest in limb-onset amyotrophic lateral sclerosis. Front Syst Neurosci. 2010; 4:158. [PubMed: 21228916]
14. Cedarbaum JM, Stambler N, Malta E, et al. The ALSFRS-R: a revised ALS functional rating scale that incorporates assessments of respiratory function. BDNF ALS Study Group (Phase III). J Neurol Sci. 1999; 169:13–21. [PubMed: 10540002]
15. Oldfield RC. The assessment and analysis of handedness: the Edinburgh Inventory. Neuropsychologia. 1971; 9:97–113. [PubMed: 5146491]
16. Basser PJ, Pierpaoli C. A simplified method to measure the diffusion tensor from seven MR images. Magn Reson Med. 1998; 39:928–934. [PubMed: 9621916]
17. Smith SM, Jenkinson M, Woolrich MW, et al. Advances in Functional and Structural MR Image Analysis and Implementation as FSL. Neuroimage. 2004; 23(Suppl 1):S208–S219. [PubMed: 15501092]
18. Jenkinson M, Beckmann CF, Behrens TEJ, Woolrich MW, Smith SM. FSL. Neuroimage. 2012; 62:782–790. [PubMed: 21979382]
19. Basser P, Jones D. Diffusion-tensor MRI: theory, experimental design and data analysis–a technical review. NMR Biomed. 2002; 15:456–467. [PubMed: 12489095]
20. Smith SM, Jenkinson M, Johansen-Berg H, et al. Tract-based spatial statistics: voxelwise analysis of multi-subject diffusion data. Neuroimage. 2006; 31:1487–1505. [PubMed: 16624579]
21. Nichols T, Holmes A. nonparametric permutation tests for functional neuroimaging: a primer with examples. Hum Brain Mapp. 2002; 15:1–25. [PubMed: 11747097]
22. Smith SM, Nichols TE. Threshold-free cluster enhancement: addressing problems of smoothing, threshold dependence and localisation in cluster inference. Neuroimage. 2009; 44:83–98. [PubMed: 18501637]
23. Chapman MC, Jelsone-Swain L, Fling BW, Johnson TD, Gruis K, Welsh RC. Corpus callosum area in amyotrophic lateral sclerosis. Amyotroph Lateral Scler. 2012:1–3.
24. Hofer S, Frahm J. Topography of the human corpus callosum revisited—comprehensive fiber tractography using diffusion tensor magnetic resonance imaging. Neuroimage. 2006; 32:989–994. [PubMed: 16854598]
25. Oishi K, Zilles K, Amunts K, et al. Human brain white matter atlas: identification and assignment of common anatomical structures in superficial white matter. Neuroimage. 2008; 43:447–457. [PubMed: 18692144]
26. Metwalli NS, Benatar M, Nair G, Usher S, Hu X, Carew JD. Utility of axial and radial diffusivity from diffusion tensor MRI as markers of neurodegeneration in amyotrophic lateral sclerosis. Brain Res. 2010; 1348:156–164. [PubMed: 20513367]
27. Carrara G, Carapelli C, Venturi F, et al. A distinct MR imaging phenotype in amyotrophic lateral sclerosis: correlation between T1 magnetization transfer contrast hyperintensity along the corticospinal tract and diffusion tensor imaging analysis. AJNR Am J Neuroradiol. 2012; 33:733–739. [PubMed: 22194369]
28. Prudlo J, Bißbort C, Glass A, et al. White matter pathology in ALS and lower motor neuron ALS variants: a diffusion tensor imaging study using tract-based spatial statistics. J Neurol. 2012; 259:1848–1859. [PubMed: 22349938]

29. Witelson SF. Hand and sex differences in the isthmus and genu of the human corpus callosum. A postmortem morphological study. Brain. 1989; 112(Pt 3):799–835. [PubMed: 2731030]

30. Wittstock M, Meister S, Walter U, Benecke R, Wolters A. Mirror movements in amyotrophic lateral sclerosis. Amyotroph Lateral Scler. 2011; 12:393–397. [PubMed: 21554031]

31. Douaud G, Filippini N, Knight S, Talbot K, Turner MR. Integration of structural and functional magnetic resonance imaging in amyotrophic lateral sclerosis. Brain. 2011; 134:3470–3479. [PubMed: 22075069]

32. Fling BW, Walsh CM, Bangert AS, Reuter-Lorenz PA, Welsh RC, Seidler RD. Differential callosal contributions to bimanual control in young and older adults. J Cogn Neurosci. 2011; 23:2171–2185. [PubMed: 20954936]

33. Song S-K, Sun S-W, Ju W-K, Lin S-J, Cross AH, Neufeld AH. Diffusion tensor imaging detects and differentiates axon and myelin degeneration in mouse optic nerve after retinal ischemia. Neuroimage. 2003; 20:1714–1722. [PubMed: 14642481]

34. Agosta F, Pagani E, Petrolini M, et al. Assessment of white matter tract damage in patients with amyotrophic lateral sclerosis: a diffusion tensor MR imaging tractography study. AJNR Am J Neuroradiol. 2010; 31:1457–1461. [PubMed: 20395382]

35. Menke RAL, Abraham I, Thiel CS, et al. Fractional anisotropy in the posterior limb of the internal capsule and prognosis in amyotrophic lateral sclerosis fractional anisotropy and ALS. Arch Neurol. 2012; 69:1493–1499. [PubMed: 22910997]

36. Foerster BR, Dwamena BA, Petrou M, Carlos RC, Callaghan BC, Pomper MG. Diagnostic accuracy using diffusion tensor imaging in the diagnosis of ALS: a meta-analysis. Acad Radiol. 2012; 19:1075–1086. [PubMed: 22749050]

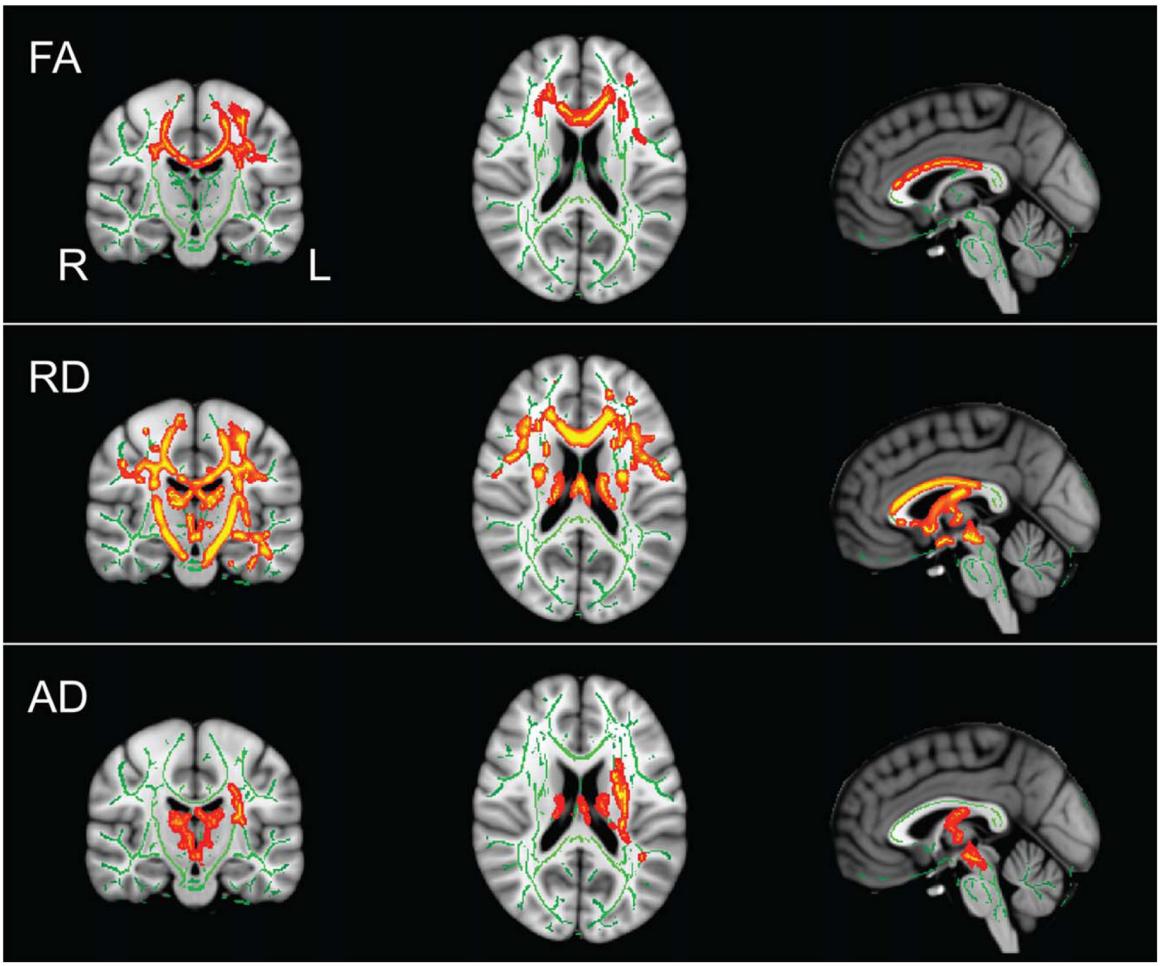

Figure 1.
DTI TBSS *P* value maps fully corrected for multiple comparisons of voxel-wise differences between patients and healthy controls for FA, RD, and AD. Results displayed at significant levels ($P < 0.05$, fully corrected for multiple comparisons) in Montreal Neurological Institute (MNI) standard space overlaid on the mean FA image derived from all participants. Major fiber tracts as determined by TBSS are displayed in green. Red-yellow clusters indicate locations of significant corrected differences between patients and controls ($P < 0.05$). Locations of images in standard space are X = −1, Y = −17, Z = 19, MNI mm.

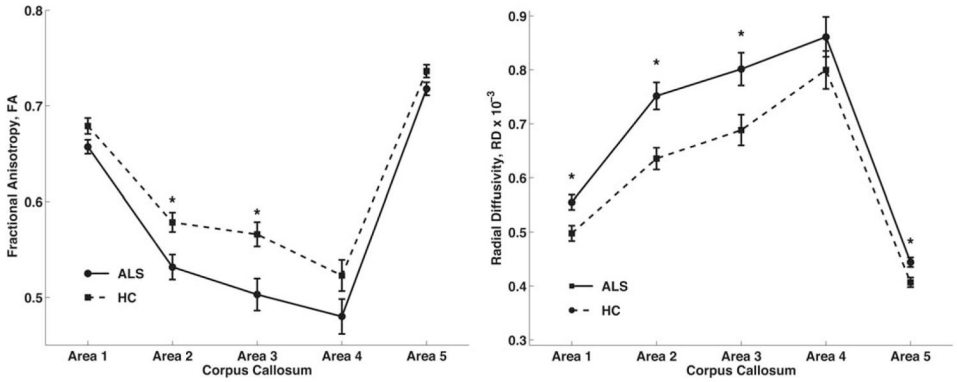

Figure 2.

Mean FA and RD values for ALS patients plotted against the control group's mean FA and RD values for each CC area (1–5). For both DTI measures, there was a significant effect between-group membership and location in the CC, and post hoc t-tests comparing groups by individual CC area that resulted in significant differences with Bonferroni correction are indicated with an asterisk (*, P <0.01).

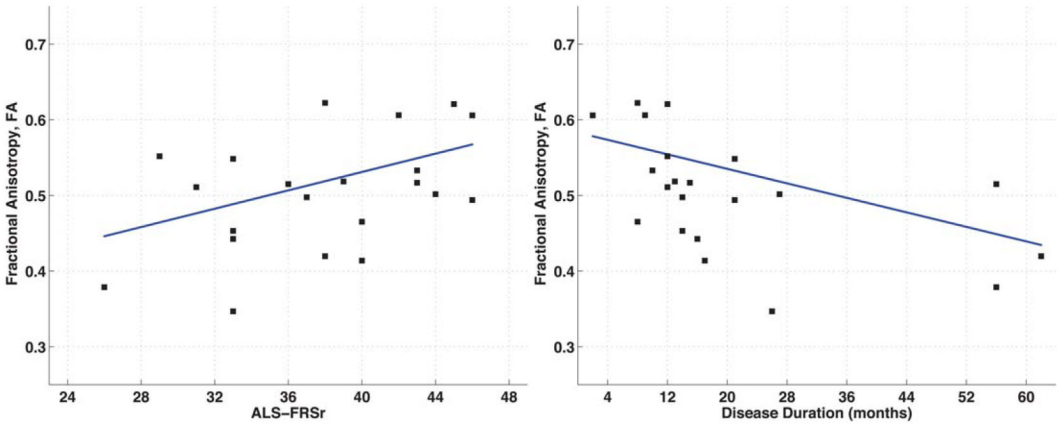

Figure 3.

Scatterplots showing significant partial correlations between mean FA in Area III of the CC and ALSFRS-r scores when correcting for age ($r = 0.457$, $P = 0.043$) and months since symptom onset when correcting for age ($r = -0.524$; $P = 0.018$). [Color figure can be viewed in the online issue, which is available at wileyonlinelibrary.com.]

Table 1

Mean Demographics Values for Patient (ALS) and Healthy Control (HC) Groups

Subject	Gender	Age (y)	Handedness	Dominant H.S. (kg)	ND H.S. (kg)	Disease duration (mo)	ALSFRS-r
ALS (n= 21)	13 M, 8 F	59.8 (± 6.5, 45.9–68.5)	20R, 1L	19.05 (0–48.94)	16.36 (0–42.42)	20.48 (±16.82)	37.86 (±5.77, 26–46)
HC (n= 21)	11 M, 10 F	56.5 (± 5.1, 44.2–63.7)	17R, 4L	34.46 (14.39–60.45)	35.23 (12.57–56.21)	N/A	N/A

H.S. = hand strength. ND H.S. = non-dominant hand strength; ALSFRS-r = ALS functional rating scale, revised version (total possible score is 48).

Table 2

Individual ALS Patient Demographic Information

	Sex	Age (y)	Hand	H.S.D. (kg)	Onset location	ALSFRS-r	DD (mo)
1	M	65.1	R	0.61	UEs	29	12.07
2	F	56.5	R	2.28	Left LE	33	26.07
3	M	60.6	R	14.39	Left LE	44	26.97
4	M	58.1	R	11.52	Bulbar	40	16.67
5	F	68.5	R	3.63	Bulbar	37	14.00
6	F	61.4	R	10.61	UE & LE	42	9.46
7	M	55.5	R	9.09	Right UE	43	14.73
8	F	67.8	R	0.76	Bulbar	43	10.17
9	F	65.8	R	7.42	Left LE	33	15.90
10	M	66.8	R	3.03	LEs	40	7.77
11	M	51.9	R	12.88	Left UE	31	11.80
12	M	64.8	R	N/A[a]	Right LE	45	12.07
13	M	56.7	R	0.75	Bulbar	39	13.17
14	M	58.3	R	10.61	Right UE	46	20.77
15	F	45.9	R[b]	4.85	Left UE	33	13.63
16	M	63.8	L[c]	0	UEs	33	21.03
17	M	63.3	R	5.75	LEs	38	61.70
18	F	65.9	R	4.40	Bulbar	26	56.17
19	M	47.1	R	6.51	UEs	36	56.20
20	F	55.3	R	25.00	Left UE	46	1.73
21	M	56.1	R	13.78	Left UE	38	7.80

[a] Hand strength could not be obtained for Subject 12 at the time of scanning.

[b] Subject 15 reported left-handedness before disease onset, but due to weakness used the right hand at the time of the scan. This patient was considered left-handed according to the Edinburgh Inventory (13).

[c] Subject 16 reported right-handedness before disease onset, but due to weakness used the left hand at the time of the scan. This patient was considered right-handed according to the Edinburgh Inventory (13).

H.S.D. = hand strength disparity; ALSFRS-r = ALS functional rating scale, revised version (total possible score is 48); DD = disease duration, defined as months between symptom onset and testing date; UE = upper extremity; LE = lower extremity.